Measurement of conversion coefficients in normal and triaxial strongly deformed bands in ^{167}Lu

G. Gürdal,[1,2,*] C. W. Beausang,[1,3,†] D. S. Brenner,[1,2] H. Ai,[1] R. F. Casten,[1] B. Crider,[3,‡] A. Heinz,[1] E. Williams,[1] D. J. Hartley,[4] M. P. Carpenter,[5] A. A. Hecht,[5,6] R. V. F. Janssens,[5] T. Lauritsen,[5] C. J. Lister,[5] R. Raabe,[3] D. Seweryniak,[5] S. Zhu,[5] and J. X. Saladin[7]

[1]*WNSL, Yale University, New Haven, Connecticut 06520-8124, USA*
[2]*Clark University, Worcester, Massachusetts 01610, USA*
[3]*University of Richmond, Richmond, Virginia 23173, USA*
[4]*United States Naval Academy, Annapolis, Maryland 21402, USA*
[5]*Argonne National Laboratory, Argonne, Illinois 60439, USA*
[6]*University of Maryland, College Park, Maryland 20742-4454, USA*
[7]*Physics and Astronomy Department, University of Pittsburgh, Pennsylvania 15260, USA*

(Received 20 November 2007; published 27 February 2008)

Internal conversion coefficients have been measured for transitions in both normal deformed and triaxial strongly deformed bands in ^{167}Lu using the Gammasphere and ICE Ball spectrometers. The results for all in-band transitions are consistent with $E2$ multipolarity. Upper limits are determined for the internal conversion coefficients for linking transitions between TSD Band 2 and TSD Band 1, the $n_w = 1$ and $n_w = 0$ wobbling bands, respectively.

DOI: 10.1103/PhysRevC.77.024314 PACS number(s): 23.20.Nx, 27.70.+q, 29.30.Ep

I. INTRODUCTION

The search for stable triaxial-deformed nuclei, rather than γ-soft nuclei, has been ongoing for many years. Despite many experiments and much theoretical effort, a unique signature for stable triaxial deformation has proved elusive. Recently, however, evidence has been found for the long predicted wobbling mode [1], which is a signature of a stable triaxial nuclear shape (a possible alternative explanation is given in Ref. [2]). The experimental evidence consists of pairs (or, in the case of ^{163}Lu, a triplet) of triaxial strongly deformed bands (TSDs) in ^{161}Lu, ^{163}Lu, ^{165}Lu, and ^{167}Lu, which show many of the characteristics expected of the wobbling mode [3–8]. These special TSD band-sets in Lu nuclei form a subset of a larger island of TSD bands in the mass $A \sim 170$ region [7,9,10]. To date, a total of ∼45 proposed TSD bands [11–13] have been observed in this region. But of all these bands, only the four Lu sets show the features expected of the wobbling mode. These features include a similar intrinsic structure, the same relative parity, an almost constant relative excitation energy, and strong interband linking transitions of mixed $M1/E2$ character, which connect states differing in spin by one unit.

In the bands in ^{161,163,165}Lu and ^{167}Lu, the excited TSD band indeed appears to have a similar intrinsic structure (based, for example, on the similarity of the dynamical moments of inertia of the bands). The excited band decays into the lower-lying band by a set of $\Delta I = 1$ nonstretched, mixed $M1/E2$ transitions with a proportionally large $E2$ content. These transitions connect states of spin I to spin $I - 1$. Generally, the interband linking transitions are found to have similar energies (for example, in ^{167}Lu, ∼700 keV).

The "gold standard" for the wobbling mode is the ^{163}Lu nucleus, where bands based on the $n = 0$, 1, and 2 wobbling phonons have been identified [4,5]. This identification is based on the observed decay pattern, in which the $n_w = 2$ wobbling band decays to the $n_w = 1$ band, and the $n_w = 1$ band decays to the $n_w = 0$ band, and on the γ-ray angular correlation measurements, which identify the linking transitions as predominantly $E2$ in character. Similar measurements, including γ-ray polarization, have been reported for ^{165}Lu [6].

More recently [7], a pair of bands in ^{167}Lu, labeled TSD Bands 1 and 2 in the partial level scheme shown in Fig. 1, have been assigned as the ground ($n_w = 0$) and first excited ($n_w = 1$) wobbling bands, respectively. Figure 1, which is a partial level scheme of ^{167}Lu, also shows other bands that are relevant to our discussion. As can be seen, TSD Band 2 decays to levels in the lower-lying TSD Band 1 via a series of six $\Delta I = 1$ transitions, each with energy of about 700 keV. The assignment of TSD Band 2 as a wobbling phonon excitation based on TSD Band 1 follows from the decay pattern of the TSD Band 2 levels, the mixed $\Delta I = 1 M1/E2$ character (with strong $E2$ component) of the transitions linking TSD Band 2 to TSD Band 1, and the measured in-band/out-of-band branching ratios. The relative spin assignments for the ^{167}Lu bands and the characterization of the linking transitions as mixed $M1/E2$ are based on angular correlation measurements, which are difficult to carry out and sometimes subject to ambiguities. Lifetime measurements, made using the Doppler shift attenuation method, indicate that the deformations of the TSD Band 1 and TSD Band 2 are considerably smaller than those observed in TSD bands in ^{163,165}Lu but are larger than those found in normal deformed (ND) bands in ^{167}Lu [14,15]. The aims of the current experiment were to measure the internal conversion coefficients of ND and TSD intra- and interband (linking) transitions in ^{167}Lu. Hence, we hoped to

*Present address: Physics Department, Rutgers University, Piscataway, New Jersey.
†cbeausan@richmond.edu
‡Present address: Physics Department, University of Kentucky, Lexington, Kentucky.

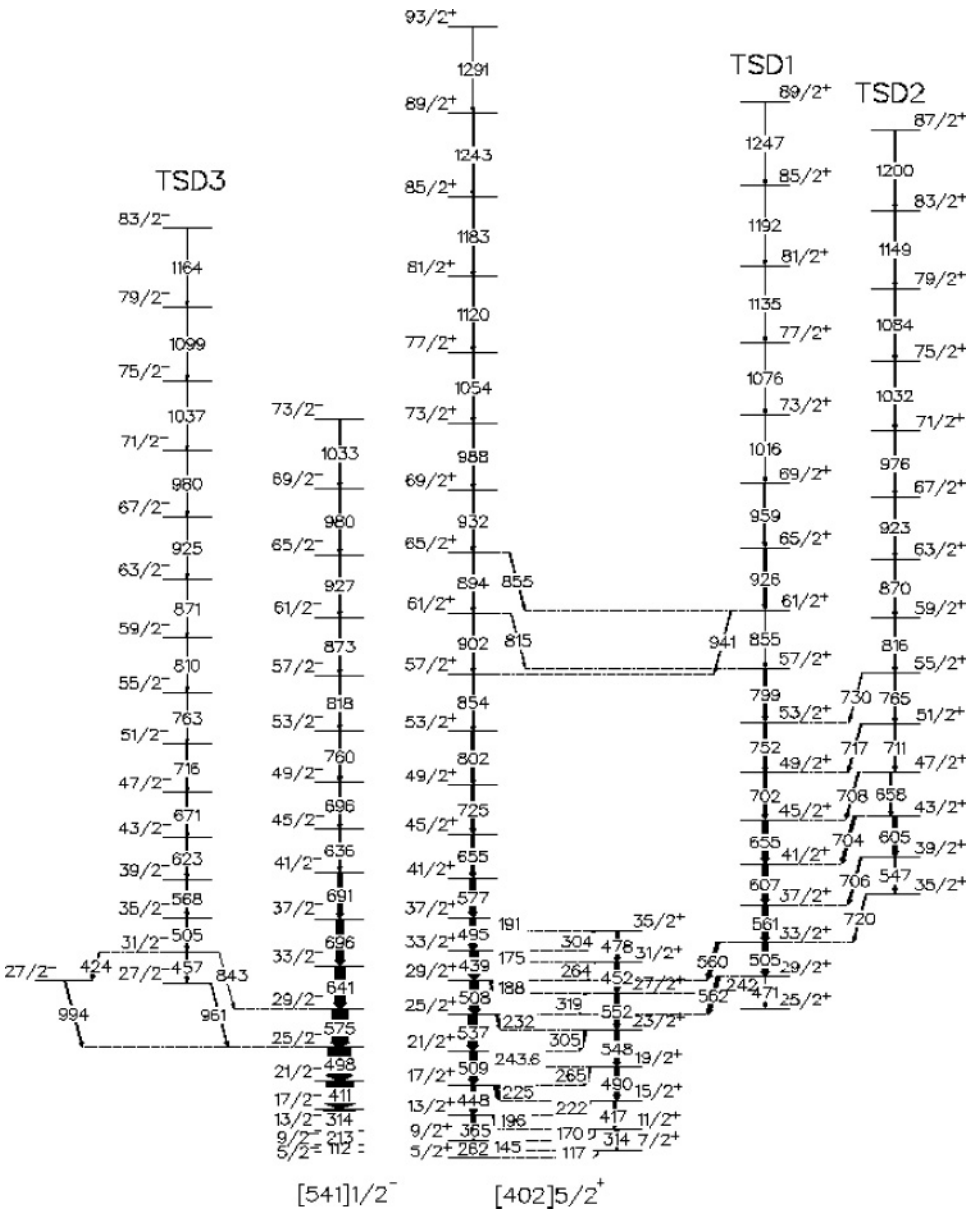

FIG. 1. Partial level scheme for ^{167}Lu showing TSD Bands 1 and 2 on the right-hand side. TSD Band 2 is a candidate for a one-phonon wobbling mode vibration built on TSD Band 1 [7]. The ∼700-keV linking transitions have been assigned $E2$ character. TSD Band 3 is shown on the left-hand side. The figure is modified from Ref. [7].

independently confirm the predominant $E2$ character of the linking transitions between TSD Band 2 and TSD Band 1 and thus provide a direct and unambiguous confirmation of the electromagnetic character of these transitions.

II. EXPERIMENTAL METHOD

High-spin states in ^{167}Lu were populated following the ^{123}Sb (^{48}Ca,4n) reaction at a beam energy of 203 MeV. The ^{123}Sb target was self-supporting and ∼1.2 mg/cm^2 thick. The ^{48}Ca beam was provided by the ATLAS accelerator at Argonne National Laboratory.

The Gammasphere [16,17] spectrometer, consisting of 101 Compton-suppressed Ge detectors for this experiment, was used to measure γ rays while coincident electrons were detected using the Internal Conversion Electron (ICE Ball) spectrometer. The ICE Ball spectrometer [18] is a Gammasphere auxiliary detector consisting of six mini-orange electron spectrometers. Each mini-orange spectrometer consists of a heavy-metal cylindrical (∼1 cm diameter and 2 cm long) plug surrounded by several permanent samarium cobalt magnets arranged so as to produce an approximately torroidal magnetic field. The concept is illustrated in Fig. 2(a). Although direct radiation (γ or charged particle) from the target is blocked by the heavy-metal plug, electrons originating at the target position are transported by the magnetic field around this plug where they are incident on a cooled Si(Li) detector that measures their energy with high resolution. Each Si(Li) detector had a diameter of ∼2.5 cm and was ∼5 mm thick. The transmission efficiency of the mini-orange spectrometer can easily be adjusted by adjusting the strength and arrangement (or simply the number) of the permanent magnets. Mini-oranges with three, five, and six magnets were utilized in this experiment. The transmission efficiencies of four of the mini-orange spectrometers were optimized for 600- to 900-keV

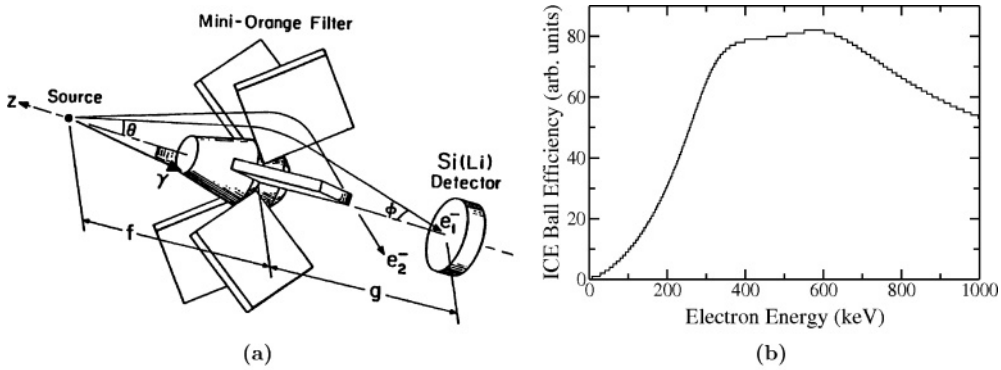

FIG. 2. (a) A schematic view of electron transmission of a mini-orange spectrometer (taken from Ref. [18]). (b) The measured transmission efficiency of the ICE Ball mini-orange spectrometers used in the current experiment plotted as a function of electron energy. As can be seen, the transmission efficiency of the spectrometers was maximum and approximately constant for electrons with energies between 300 and 700 keV. The K internal conversion electrons from the linking transitions of interest have energies of ∼640 keV, whereas the TSD intraband transitions range upwards from ∼400 keV.

electrons. The transmission efficiencies of the remaining two spectrometers (those with only three magnets) were optimized for lower energy electrons. During the course of the experiment, technical difficulties resulted in only four mini-orange channels working correctly. The combined relative transmission efficiency of these four detectors, measured using a standard ^{152}Eu electron source, is presented in Fig. 2(b). As can be seen, the transmission efficiency is at its largest value and is approximately constant, for the energies of interest, i.e., for electrons with energies from ∼300 to 700 keV. The K internal conversion electrons from the intraband transitions in the TSD bands range in energy from ∼400 keV up to ∼1000 MeV, whereas those from the interband linking transitions have energies of ∼640 keV. Thus, the transmission of ICE Ball was optimized for these transitions. For higher-energy electrons, the transmission efficiency slowly decreases. For lower-energy electrons, the transmission drops rapidly. The low transmission efficiency at low electron energies is intended to reduce the very large background from δ electrons that are produced in copious quantities when the ^{48}Ca beam impinges on the target.

The energy resolution of the Si(Li) detectors was measured using standard calibration sources both before and after the experiment and was found to be between 3 and 7 keV FWHM depending on the electron energy and specific detector. A typical spectrum obtained using a ^{207}Bi source is reproduced in Fig. 3. However, in-beam the electron energy resolution obtained was ∼20 keV and was dominated by Doppler broadening effects due to the high recoil velocity (∼2.4% the speed of light) and the large opening angle of the mini-orange spectrometers.

The master trigger for the data acquisition required a prompt coincidence between either five or more Compton suppressed Ge detectors or at least one Si(Li) detector in ICE Ball plus at least two Compton suppressed Ge detectors. Over a 10-day period a total of $\sim 2 \times 10^9$ events were recorded, the data being about equally split between pure γ-γ and e-γ coincidences. Additional details of the experimental setup can be found in Ref. [15].

Figure 4 shows the total projection of the in-beam electron spectrum and illustrates some of the challenges inherent to in-beam conversion electron spectroscopy: the spectrum has a very large continuous background, particularly at low energies, primarily due to beam-induced δ electrons. The discrete-energy electron-peaks, due to internal conversion, appear as small bumps superimposed on this background. To clean up the spectrum and to eliminate contaminants due to the many doublet transitions in ^{167}Lu (over 300 γ-ray transitions have so far been assigned to this nucleus), a triples analysis was performed. After unfolding triple- and higher-fold coincidence data, asymmetric γ-γ-γ and γ-γ-e half cubes were created. In the subsequent analysis, pairs of peak coincident gates were set on the γ-ray axes and the resulting spectrum (either γ or electron) was examined. Identical gating and background subtraction procedures were used for both γ and electron half cubes. In general, the resulting spectra were very clean.

For example, Fig. 5 shows double-gated γ-ray and electron spectra for the [541]1/2 normal deformed band in ^{167}Lu. The spectra result from summing all pairs of gates placed on

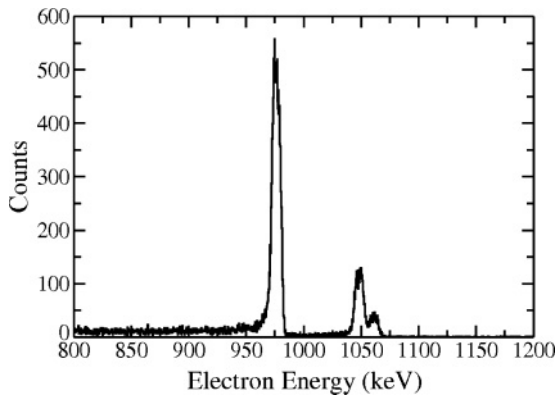

FIG. 3. A typical electron calibration spectrum obtained using a ^{207}Bi source. The figure shows the portion of the spectrum in the vicinity of the K, L, and M conversion peaks from the 1086-keV transition.

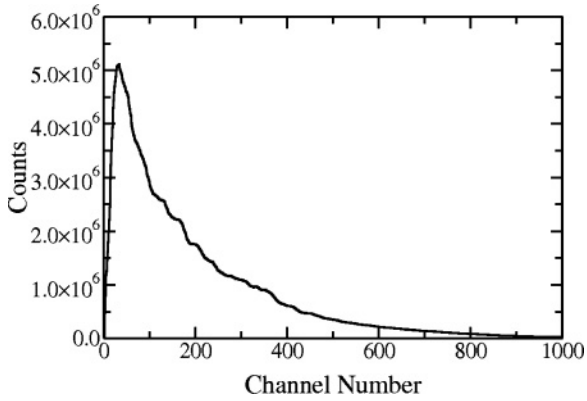

FIG. 4. Total projection of the in-beam electron spectrum illustrating the large continuous background (primarily due to beam-induced δ rays) with much weaker discrete peaks (from internal conversion electrons) superimposed.

15 transitions in the band, ranging in energy from 213 to 980 keV, a total of 105 gate-pairs. As can be seen, the γ-ray spectrum is extremely clean and contaminant free. In particular, note that there are well in excess of 10^6 counts in individual γ-ray peaks.

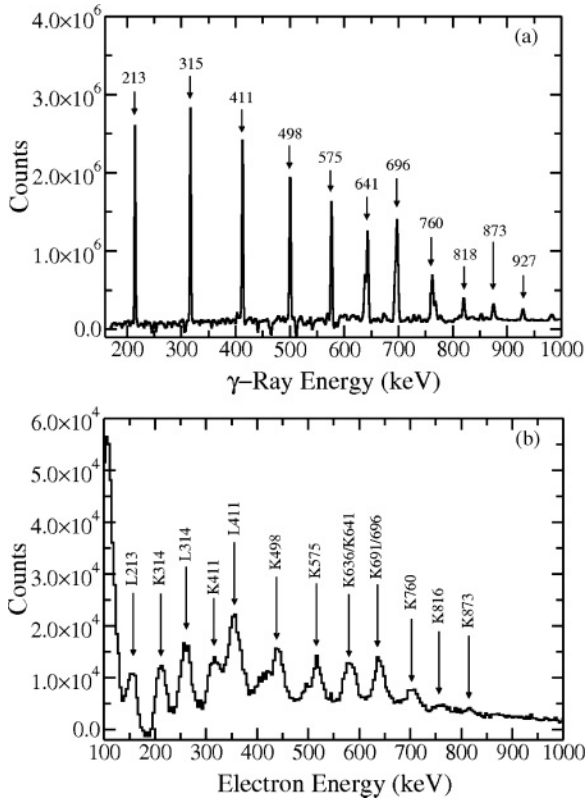

FIG. 5. Double gated (a) γ-ray spectrum and (b) electron spectrum for the [541]1/2 normal deformed band in ^{167}Lu . The spectra are the sum of all pairs of double gates on transitions in the [541]1/2 band from 213 to 980 keV (a total of 105 gate pairs). The arrows and labels indicate the approximate positions of the γ rays and corresponding K and L conversion peaks from the band members.

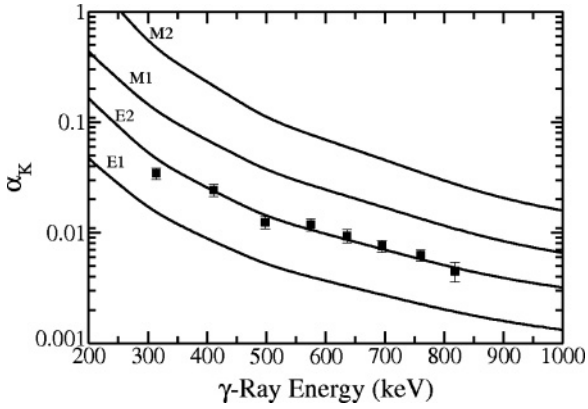

FIG. 6. Measured conversion coefficients for in-band transitions in the [541]1/2 band of ^{167}Lu .

The corresponding electron spectrum is given in Fig. 5(b). Although identical gating procedures were used, the poorer electron energy resolution and the fact that each γ-ray transition has conversion peaks corresponding to electrons being ejected from both the K and L shells (and weaker M and N) ensures that there are many overlapping peaks in Fig. 5(b). Although accounting for these doublets complicates the analysis somewhat, conversion measurements can still be obtained.

The internal conversion coefficient, α, is defined as

$$\alpha = \frac{I_e}{I_\gamma} = \frac{N_e}{N_\gamma} \times \frac{\epsilon_\gamma}{\epsilon_e} \times k, \qquad (1)$$

where the subscripts e and γ refer to electrons and γ rays, respectively. In this equation, I refers to the measured intensities obtained from the corresponding γ-ray or electron spectrum by dividing the measured peak areas N by their corresponding peak detection efficiencies ε. The coefficient k is an energy-independent constant that serves to normalize the (relative) efficiencies of Gammasphere and ICE Ball. Initially, the value of k was obtained by insisting that the K conversion coefficient for the 411-keV transition in the [541]1/2 band agree with the expected $E2$ value. As Fig. 6 shows, the conversion coefficients for all of the other in-band transitions are in excellent agreement with E2 multipolarity, as expected for members of a rotational band. This agreement is gratifying, as it implies that the normalization coefficient k is indeed energy independent and that the measured shapes of both the Gammasphere and ICE Ball efficiency curves are accurate over the entire energy range covered by this band. Having ensured this, the value of k was adjusted to obtain the best agreement for all members of the [541]1/2 band, and this value was used in the subsequent analysis for the other ND and for the TSD bands. The required adjustment was only on the order of a few percent.

Figure 6 shows the extracted α_K conversion coefficients for eight transitions (ranging in energy from 300 to 800 keV) in the [541]1/2 band using the data shown in Figs. 5(a) and 5(b). As can be seen, the data are in excellent agreement with the expected $E2$ nature for all the transitions. As an additional test of the analysis method, conversion coefficients were also extracted for several $\Delta I = 2$ members of the

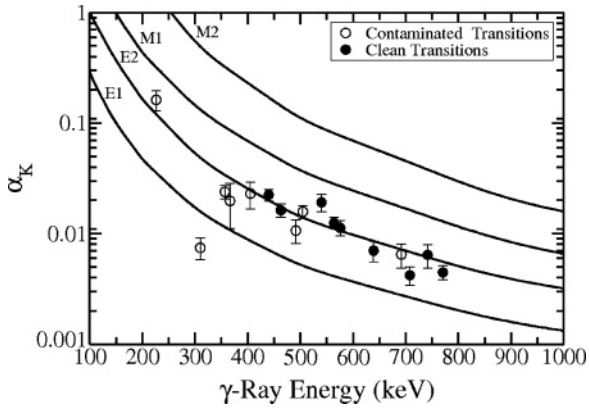

FIG. 7. Measured K conversion coefficients for the ground-state band compared to theoretical values for $E1$, $E2$, $M1$, and $M2$.

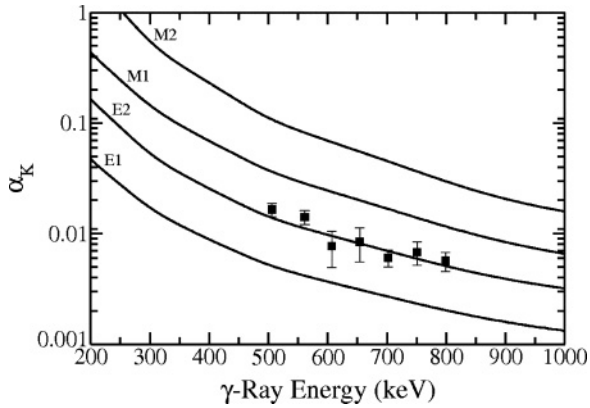

FIG. 9. Measured K conversion coefficients for TSD Band 1 compared to theoretical values for $E1$, $E2$, $M1$, and $M2$ multipolarity.

ground-state normal deformed band in ^{167}Lu. Figure 7 provides the results for the ground-state band. As expected, the results are consistent with $E2$ multipolarity for these transitions.

Moving to the triaxial strongly deformed bands, Fig. 8 shows double-gated γ-ray and electron spectra for TSD Band 1. To generate these spectra, gates were placed on 13 members of TSD Band 1 ranging in energy from 505 to 1135 keV, a total of 78 gate pairs. As can be seen, the quality of the spectra is high. Conversion electron peaks for several of the TSD band transitions are clearly identifiable, as are those for the lower-lying normal deformed transitions fed by TSD Band 1. The peak areas in Fig. 8, compared to those

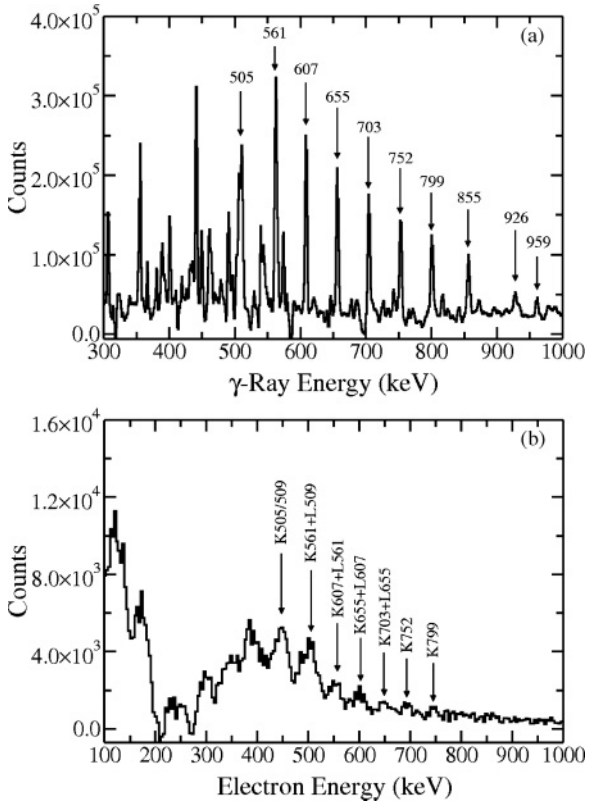

FIG. 8. Double gated (a) γ-ray spectrum and (b) electron spectrum for TSD Band 1 in ^{167}Lu.

in Fig. 5, are consistent with this reduction in the number of available gate pairs and with the published intensity for TSD Band 1, ∼10% of the normal deformed [541]1/2 band. Figures 8(a) and 8(b) still have ample statistics to allow the extraction of conversion coefficients and these are plotted in Fig. 9 for seven members of TSD Band 1. The results are in excellent agreement with $E2$ multipolarity for all of the in-band transitions.

The published intensity of TSD Band 2, the one-phonon wobbling band, is ∼5% or roughly half that of TSD Band 1 [7]. However, many of its transitions are close doublets with much more intense transitions elsewhere in the level scheme or in TSD Band 1. For example, there are close-lying doublets with energies of 605 keV $43/2 \rightarrow 39/2$ (TSD Band 2) and 607 keV $41/2 \rightarrow 37/2$ (TSD Band 1), 658 keV $47/2 \rightarrow 43/2$ (TSD Band 2) and 655 keV $45/2 \rightarrow 41/2$ (TSD Band 1), and 547 keV $39/3 \rightarrow 35/2$ (TSD Band 2) and 552 keV $27/2 \rightarrow 23/2$ and 548 keV $23/2 \rightarrow 19/2$ ([402]5/2 band) to name but a few. As a result, both the number of gate pairs available for generating the electron and γ spectra and the useful width of the gates were limited. In the end, all combinations of 12 gates were utilized, a total of 66 pairs, but, as pointed out, to maintain the cleanliness of the spectra several of these were narrower than optimum. To increase the final statistics, additional gates, requiring one clean transition in TSD Band 2 and one of the 505-, 607-, or 655-keV transitions in TSD Band 1, fed by TSD Band 2, were added to the gating condition. The final spectra for γ rays and electrons for TSD Band 2 are shown in Figs. 10(a) and 10(b), respectively. Due to the limited number of gate pairs, the narrowness of the gates themselves, and the already reduced intensity of TSD Band 2 compared to TSD Band 1, the statistics in the resulting spectra are very limited.

A quick examination of the vertical scale in Fig. 10 indicates that the statistics are much reduced, by roughly a factor of 10, compared to the TSD Band 1 spectra. In the γ-ray spectrum, Fig. 10(a), the in-band transitions in TSD Band 2 are clearly visible, as are the 505-, 561-, 607-, and 655-keV members of TSD Band 1 fed by decays from TSD Band 2. Indeed, the sought after 704–706–708 complex of interband linking transitions is clearly visible in Fig. 10(a) to the left of the 711-keV TSD Band 2 transition (the 717-, 720-, and 730-keV linking transitions are much weaker in

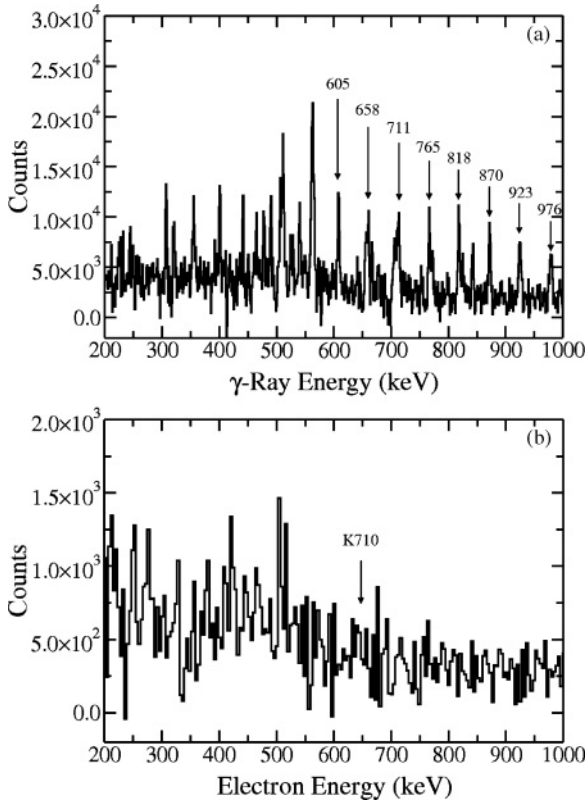

FIG. 10. Double gated (a) γ-ray spectrum and (b) electron spectrum for TSD Band 2.

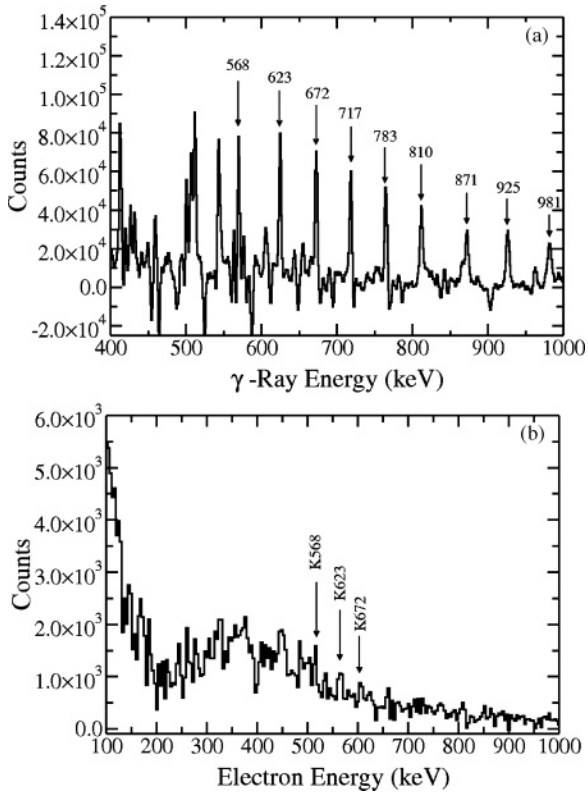

FIG. 11. Double gated (a) γ-ray spectrum and (b) electron spectrum for TSD Band 3.

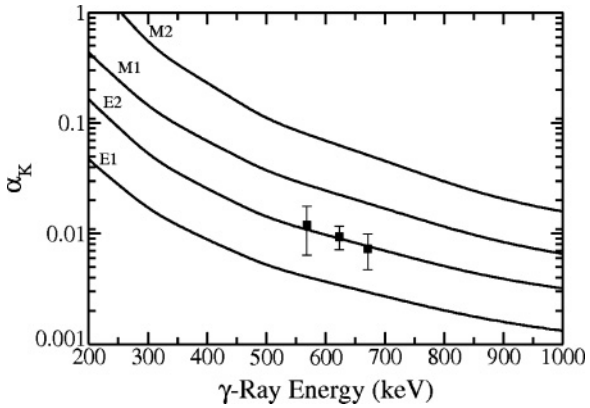

FIG. 12. Measured K conversion coefficients for TSD Band 3 compared to theoretical values for $E1$, $E2$, $M1$, and $M2$ multipolarity.

Fig. 10(a), due both to the gating conditions that emphasize the 706 complex and, presumably, the inherent weakness of these branches). Unfortunately, this level of statistics is not sufficient to allow any useful information to be extracted from the electron spectrum, Fig. 10(b). The arrow indicates the expected position for K conversion electrons from the 706-keV complex and the 711-keV in-band $E2$ transition. A fit to this region of the spectrum yields an upper limit on the conversion coefficient. For this fit, the known electron peak-shape parameters (determined from electron peaks in the ND and TSD Band 1) were used while the centroid was fixed at the expected position. Thus, the peak area was the only free parameter. The most likely value of α_K determined in this manner is 0.008, close to the expected $E2$ value with very large uncertainty ($\sim$0.06). Thus we can present only an upper limit of $\alpha_K < 0.07$, which is not low enough to rule out any likely multipolarity for the linking transition.

Finally, Fig. 11 presents double-gated spectra for TSD Band 3. As for TSD Band 2 spectra are combinations of two sets of gating conditions, the first requiring all combinations of double gate pairs on "clean" transitions in TSD Band 3, the second requiring a coincidence between one transition in the band and a transition in the ND states below. As can be seen the quality of the resulting spectra is reasonable and allow the extraction of α_K for three transitions in TSD Band 3, as given in Fig. 12. These conversion coefficients are consistent with the expected $E2$ multipolarity.

III. CONCLUSION

In conclusion, internal conversion coefficients have been measured for many transitions in both normal-deformed and triaxial strongly deformed bands in ^{167}Lu. The results for all of the in-band transitions are consistent with the expected $E2$ multipolarity. Although we were able to extract a limit for α_K for the interband linking transitions between TSD Bands 2 and 1, the limit, $\alpha_K < 0.07$ is not sufficient to allow us to make any statement about the multipolarity of these transitions or to rule out any likely multipolarity. The primary reasons for the large limit for α_K for the linking transitions lie in the weakness of intensity of TSD Band 2 and in the contamination of many

of its transitions with much more intense transitions in normal deformed or other TSD bands.

ACKNOWLEDGMENTS

This experiment would not have been possible without the help of the many superb professionals at the ATLAS accelerator at Argonne National Laboratory. The invaluable assistance of these many individuals is gratefully acknowledged. This work was supported by the U.S. Department of Energy, Office of Nuclear Physics, under grants DE-FG02-88ER40417, DE-FG02-91ER-40609, DE-FG02-05ER41379, and DE-AC02-06CH11357; by the U.S. Department of Energy National Nuclear Security Administration under grant number DE-FG52-06NA26206; and by the National Science Foundation under grant number PHY-0554762.

[1] A. Bohr and B. R. Mottelson, *Nuclear Structure* (W. A. Benjamin, New York, 1975), Vol. II.
[2] R. F. Casten, E. A. McCutchan, N. V. Zamfir, C. W. Beausang, and J.-Y. Zhang, Phys. Rev. C **67**, 064306 (2003).
[3] P. Bringel, H. Hübel, H. Amro, M. Axiotis, D. Bazzacco, S. Bhattacharya, R. Bhowmik, J. Domscheit, G. B. Hagemann, D. R. Jensen *et al*., Eur. Phys. J. A **16**, 155 (2003).
[4] S. W. Ødegård, G. B. Hagemann, D. R. Jensen, M. Bergström, B. Herskind, G. Sletten, S. Törmänen, J. N. Wilson, P. O. Tjøm, I. Hamamoto *et al*., Phys. Rev. Lett. **86**, 5866 (2001).
[5] D. R. Jensen, G. B. Hagemann, I. Hamamoto, S. W. Ødegård, B. Herskind, G. Sletten, J. N. Wilson, K. Spohr, H. Hübel, P. Bringel *et al*., Phys. Rev. Lett. **89**, 142503 (2002).
[6] G. Schönwaßer, H. Hübel, G. B. Hagemann, P. Bednarczyk, G. Benzoni, A. Bracco, P. Bringel, R. Chapman, D. Curien, J. Domscheit *et al*., Phys. Lett. **B552**, 9 (2003).
[7] H. Amro, W. C. Ma, G. B. Hagemann, R. M. Diamond, J. Domscheit, P. Fallon, A. Görgen, B. Herskind, H. Hübel, D. R. Jensen *et al*., Phys. Lett. **B553**, 197 (2003).
[8] I. Hamamoto, Phys. Rev. C **65**, 044305 (2002).
[9] C.-H. Yu, G. B. Hagemann, J. M. Espino, K. Furuno, J. Garrett, R. Chapman, D. Clarke, F. Khazaie, J. C. Lisle, J. N. Mo *et al*., Nucl. Phys. **A511**, 157 (1990).
[10] Y. R. Shimizu, M. Matsuzaki, and K. Matsuyanagi, Phys. Rev. C **72**, 014306 (2005).
[11] H. Amro, P. G. Varmette, W. C. Ma, B. Herskind, G. B. Hagemann, G. Sletten, R. V. F. Janssens, M. Bergström, A. Bracco, M. Carpenter *et al*., Phys. Lett. **B506**, 39 (2001).
[12] A. Neußer-Neffgen, H. Hübel, P. Bringel, J. Domscheit, E. Mergel, N. Nenoff, A. K. Singh, G. B. Hagemann, D. R. Jensen, S. Bhattacharya *et al*., Phys. Rev. C **73**, 034309 (2006).
[13] D. J. Hartley, M. K. Djongolov, L. L. Riedinger, G. B. Hagemann, R. V. F. Janssens, F. G. Kondev, E. F. Moore, M. A. Riley, A. Aguilar, C. R. Bingham *et al*., Phys. Lett. **B608**, 31 (2005).
[14] G. Gürdal, H. Amro, C. W. Beausang, D. S. Brenner, M. P. Carpenter, R. F. Casten, C. Engelhardt, G. B. Hagemann, C. R. Hansen, D. J. Hartley *et al*., J. Phys. G **31**, S1563 (2005).
[15] G. Gürdal, Ph. D. thesis, Clark University, 2007.
[16] I.-Y. Lee, Nucl. Phys. **A520**, 641c (1990).
[17] R. V. F. Janssens and F. S. Stephens, Nucl. Phys. News **6**, 9 (1996).
[18] M. Metlay, J. X. Saladin, I. Y. Lee, and O. Dietzsch, Nucl. Instrum. Methods A **336**, 162 (1993).